Dual Chemically Synthesized Tin (IV) Di-lead Tetraoxide (SnPb$_2$O$_4$) Alloyed Thin Films

Joseph Ijeoma Onwuemeka

Imo State University, Owerri, Nigeria

Abstract:- **SnPb$_2$O$_4$, alloyed thin films were successfully deposited on glass substrates using dual solution synthesis under the deposition condition of 60°C of NaOH solution. The deposited alloyed samples were annealed between 100°C to 250°C using Master Chef Annealing Machine. The crystallographic studies were done using X-ray diffractometer (XRD) and scanning electron microscope (SEM). The XRD pattern of SnPb$_2$O$_4$ alloyed thin films of samples A$_{11}$ and A$_{12}$ with one diffraction peak at 2θ = 22.30^0 with corresponding Miller indices (111) and the grain size of the alloys is 92.29nm. SEM results show that sample A$_{11}$ and A$_{12}$ have high porosity and roughness which may be due to vaporization of water. Rutherford backscattering Spectroscopy (RBS) analysis confirmed the percentage of the elements of , lead, tin, and oxygen in the alloyed thin films samples. The optical characterization was carried out using UV-1800 series, double beam spectrophotometer. Sample A$_{11}$ of SnPb$_2$O$_4$ alloyed thin films annealed at 250^{0}C, shows optical transmittance of 30%-65% in the ultraviolet region, 66%-76% in the visible, and 76%-80% in the near-infrared regions of electromagnetic spectrum. Sample A$_{12}$ annealed at 200°C has an optical transmittance of 27% -70% in the ultraviolet region, 71% -80% in the visible and 81%-86% in the near infrared regions of electromagnetic spectrum. The two samples, have direct average wide band gap of 3.65±0.05eV.**

Keywords: **optical transmittance, characterization, ultraviolet region, band gap**

I. INTRODUCTION

Materials science play a vital role in this modern age of science and technology. Various kinds of materials are used in industry, housing, agriculture, transportation, etc., to meet the plant and individual requirements. The rapid developments in the field of quantum theory of solids have opened vast opportunities for better understanding and utilization of various materials [1].

The usefulness of thin films and their applications cut across microelectronics, magnetic and gas sensors, optics, corrosion protection, wear resistance, and solar control devices among others [2].

The spectacular success in the field of space is primarily due to the rapid advances in high-temperature and high-strength materials. The electrical and optical properties of these compounds can be tuned on demand by reducing or increasing the number of layers [3], which makes them potential candidates for tunable nano electronics [4].

The primary n-type TCOs have remained virtually unchanged in the last two decades of simple oxides such as ZnO, CdO, SnO$_2$, Ga$_2$O and In$_2$O$_3$ [5] .

PbO thin films are good materials used as active layers in various types of solar cells and a passive layer in solar-selective surfaces. From literature, PbO thin films are semiconductor materials with energy band gap of 1.2- 2.2eV. The PbO films prepared under this condition is found useful as anti-dazzling coating and quality material for eye glasses, solar-thermal energy collector, selective absorbing layer, because of its high solar absorptance and low emittance [6], tint films on windscreen for cars and glass windows, solar cell applications and as a semiconductor material for electronic applications.

Alloys are made by mixing two or more elements, at least one of which is a metal. This is usually called the primary metal or the base metal, and the name of this metal may also be the name of the alloy [7]. In this respect, all the various forms of an alloy containing only two constituents, like iron and carbon, is called a binary system, while all of the alloy combinations possible with a ternary alloy, such as alloys of iron, carbon and chromium [8].

In this present work, the dual synthesis and characterization of SnPb$_2$O$_4$ alloyed thin films have been studied.

II. MATERIALS AND METHODS

2.1 Deposition of PbO Thin Films by SILAR Method

The dual approach employed in the deposition of SnPb$_2$O$_4$ involves the deposition of PbO thin films using SILAR method followed by SGT. The synthesis of PbO thin films using SILAR method constituted**:** 3ml of 3M solution of ammonia used as complexing agent and measured with a syringe and was added into separate beakers containing 16.56g of 0.2M solution of Pb(NO$_3$)$_2$ dissolved in 250cm^3 water and 16g of 2M solution of NaOH dissolved in 200cm^3 of watter, 3ml of 99% of 3M solution of ammonia used as complexing agent. The initial stage here is the formation of white precipitate and in addition of excess NH$_3$, and stirring vigorously the dissolution of the precipitate occurred leading to a complex solution called lead tetra-amine complex ion as given in equation (2.1). This reaction was made in 50ml beaker and de-ionized water was added up to 50ml in order to free the ions in the solution.

$$Pb(NO_3)_2 + 4NH_3 \longleftrightarrow [Pb(NH_3)_4]^{2+} + 2NO_3^- \quad (2.1)$$
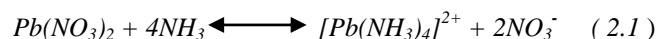
PbO thin films were deposited as given in equation, on the substrates in cycles; one cycle is completed by dipping the substrate first into the beaker containing the cationic precursor followed by rinsing in de-water for 5 seconds and finally immersing it in the third beaker of ionic precursor.

.Adsorption took place in the first beaker containing $[Pb(NH_3)_4]^{2+}_{(aq)}$ when the substrates were immersed in it for 6 seconds and then rinsed in a beaker of de-ionize water in the second beaker for 5 seconds, followed by reaction in the third beaker, containing the anionic precursor, which is 16g of 2M solution of NaOH dissolved in $200cm^3$ of water kept at constant temperature of 60^0C for 6 seconds after which the substrates were rinsed in de-ionized water for 5 seconds and this was repeated based on the number of chosen cycles and dip-time for the samples as depicts in Table 3.1. The reaction equation for SILAR deposition of PbO thin films is given in equation (2.2).
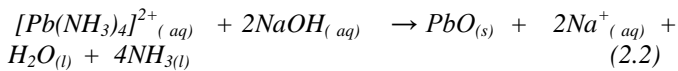
$$[Pb(NH_3)_4]^{2+}_{(aq)} + 2NaOH_{(aq)} \rightarrow PbO_{(s)} + 2Na^+_{(aq)} + H_2O_{(l)} + 4NH_{3(l)} \qquad (2.2)$$

Table 2.1 The deposition of PbO thin films by SILAR Method

Sample	Dip-time(s)in each reactant	No. of cycle	Dip-time(s) in each Beaker of H₂O
A_7	6	15	5
A_8	6	15	5
A_9	6	15	5
A_{10}	6	15	5
A_{11}	6	15	5
A_{12}	6	15	5

2.2 Deposition of SnPb₂O₄ Using Solution Growth Technique

The constituent materials that make-up the deposited samples of $SnPb_2O_4$ on the substrates includes: 20ml of 13.52g of 0.24M solution of hydrated tin(II) chloride, 3ml of 3M solution of NH_3 and 15ml of 16g of 2M solution of NaOH and the substrates containing the deposited samples of suspected

PbO thin films prepared by SILAR method. Ammonia $(NH_{3(aq)})$ in this reaction is the complexing agent. It controls the rate of ion – by – ion interaction, thereby moderating the rate of formation of precipitate. It also creates an alkaline medium for good formation of deposits. The process was performed at the constant parameters such as concentration, volume of complexing agent, temperature, time of growth and pH as given in Table 3.2. By immersing the substrates containing the suspected PbO thin films in already prepared solution mixture containing 0.24M solution of hydrated tin (II) chloride complexed with NH_3 solution given in equation (2.3), and with NaOH solution as the anionic precursor and were kept for 12 hours for optimum depositions of $SnPb_2O_4$ to occur after which the samples were removed and rinsed in de-ionized water and were allowed to dry in air by hanging in slanting order by the aid of clips.

Several bath compositions were employed, but the optimum result was achieved with the specification noted above for all the samples in Table 2.2. Equally good and uniform depositions were obtained using 0.5M, 0.25M, 0.1M, 0.4M solutions of tin chloride. The solutions for the depositions were made in 50ml beakers and on glass substrates at the pH value of 10. The resultant equation from the reaction is given in equation (2.4).

$$SnCl_2.2H_2O + 4NH_3 \longleftrightarrow [Sn(NH_3)_4]^{2+} + 2H_2O + 2Cl^- \qquad (2.3)$$

$$2PbO_{(s)} + [Sn(NH_3)_4]^{2+}_{(aq)} + 4NaOH^-_{(aq)} \rightarrow SnPb_2O_{4(s)} + 4Na^+ + 2H_2O_{(l)} + 4NH_{3(aq)} \qquad (2.4)$$
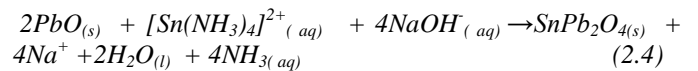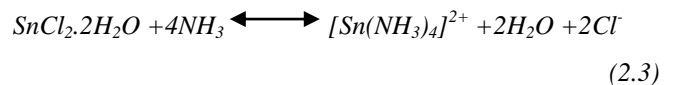
The samples were annealed at varying temperatures ranging from 100^oC-250^oC in order to remove the water of crystallization, thereby obtaining adherent white deposit on the substrates as given in equation (2.5).

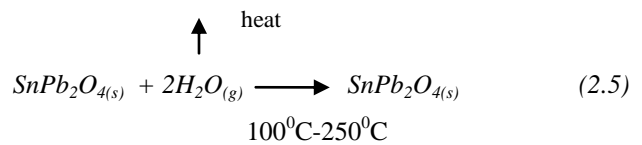$$SnPb_2O_{4(s)} + 2H_2O_{(g)} \xrightarrow{heat} SnPb_2O_{4(s)} \qquad (2.5)$$
$$100^0C\text{-}250^0C$$

Table 2.2 The different parameters for the deposition of PbO:SnO₂ thin films of 0.24M solution of SnCl₂.

Samp-les	Annealing Temp.(ºC) (for1hour)	Pb(NO₃)₂ Conc. (mol)	NH₃ Conc. (mol)	NaOH Conc. (mol)	SnCl₂ Vol. (ml)	NH₃ Vol. (ml)	NaOH Vol. (ml)	Dep.Temp (NaOH) ºC	Dep. Time (hr)
A_7	150	0.20	3.00	2.00	20.00	5.00	15.00	60.00	12.00
A_8	100	0.20	3.00	2.00	20.00	5.00	15.00	60.00	12.00
A_9	150	0.20	3.00	2.00	20.00	5.00	15.00	60.00	12.00
A_{10}	200	0.20	3.00	2.00	20.00	5.00	15.00	60.00	12.00
A_{11}	250	0.20	3.00	2.00	20.00	5.00	15.00	60.00	12.00
A_{12}	200	0.20	3.00	2.00	20.00	5.00	15.00	60.00	12.00

III. RESULTS AND DISCUSSION

It was noted that when 5ml of 3M solution of 99% NH_3 was allowed to react with 20ml of 0.2M solution of $SnCl_2$, a white precipitate was initially formed, which dissolved in excess NH_3 solution forming a colourless transparent solution of $[Sn(NH_3)_4]^{2+}$ (tetra-ammine complex tin ion). When 15ml of 1M solution of NaOH at 60^oC was added to the solution of $[Sn(NH_3)_4]^{2+}$, the white precipitate reappeared. When the substrates containing PbO thin films deposited by SILAR method were inserted into the mixture, it took 12 hours, for $SnPb_2O_4$, to deposit optimally depending on the deposition parameters such as pH, volumes of reactants and the concentrations.

It must be stated clearly here that the chosen parameters (i.e concentration, volume, temperature, pH and time of deposition) were found largely by trial and error and we have no means of guaranteeing that they lead to the best possible optical and electrical properties [10].

From literature, lead salts has the capabilities of forming complex solutions with ammonia. This makes ammonia solution a suitable complexing agent for the deposition of the above named oxide thin films.

The concentration of Pb^{2+}, decreases with increasing concentration of complexing agents.

Thus, the rates of reaction and the formation of precipitates are reduced, leading to a larger terminal thickness of the films.

It was observed that the deposition of these oxide thin films is pH-dependent. OH^- from NaOH, did not take part in the complex formation therefore, the addition of OH^- precipitated the corresponding hydrous oxides of the individual ions which were deposited on the substrates.

In the case of OH^- ions taking part in the reaction processes, its addition increases the pH value, making the complex more stable, thereby reducing the concentration of free radicals. The suitable pH value for this work is 11 as detected by the piston pH meter.

The deposited films were subjected to heat treatment from 100^oC-250^oC. using Master Chef Annealing Machine.

3.1 Characterization

It is often necessary to determine the elements that make up the thin film samples. In this work, atomic compositions and the thicknesses of the samples were determined by Rutherford Backscattering Spectroscopy, using 2.2MeV alpha beam, obtained from CERD Ion Beam Analysis (IBA) Facility With Model: NEC 5SDH 1.7 MV Pelletron Tandem Accelerator equiped with a Radio Frequency Charge Exchange Ion Source Alphatron.

The Rutherford backscattering analysis shows that the samples A_{11} and A_{12} of $SnPb_2O_4$ alloyed thin films annealed at 250^oC and 200^oC respectively have 4.82% of lead, 1.39% of tin, 93.79% of oxygen with thickness of 105.20nm and 3.47%

of lead, 1.28% of tin, 85.25% of oxygen with thickness of 109.28nm. These are shown in Figure 3.1 and Figure 3.2 and are respectively itemized in Table 3.1 and Table 3.2. These result in oxygen-rich films, which maybe as a result of exposure to air and surface hydroxide [11].
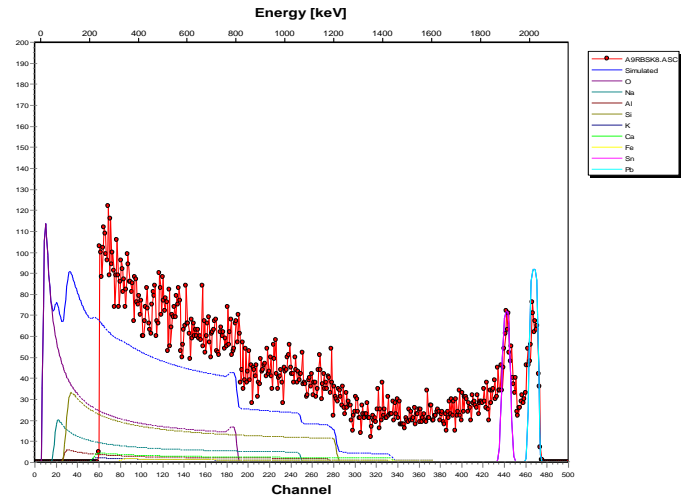

Figure 3.1 The composition of sample A_{11} of $SnPb_2O_4$ with thickness, 105.20nm as measured by Rutherford backscattering spectroscopy

Table 3.1 The elements in sample A_{11} of $SnPb_2O_4$ alloyed thin films

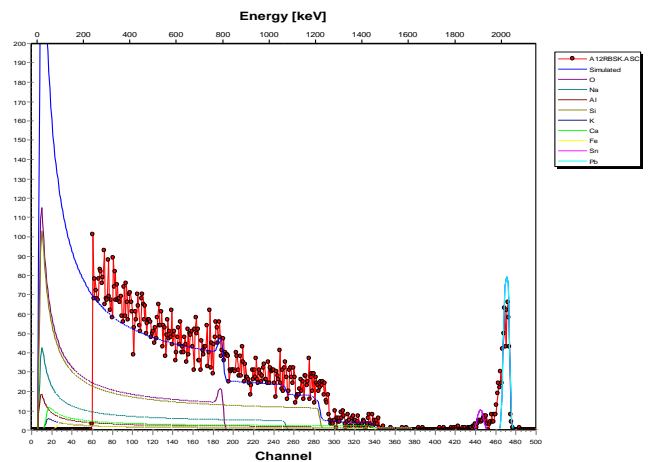| Elements	Layer(1)%Comp.	Layer(2)%Comp.
O	93.79	56.00
Ca	-	1.83
Fe	-	0.52
Na	-	12.60
Al	-	0.53
Si	-	28.00
Pb	4.82	-
Sn	1.39	

Figure 3.2 The composition of $SnPb_2O_4$ of sample A_{12} with thickness, 109.28nm as measured by Rutherford backscattering spectroscopy.

Table 3.2 The elements in sample A_{12} of $SnPb_2O_4$ alloyed thin films

Elements	Layer(1)%Comp.	Layer(2)%Comp.
O	85.25	56.00
Ca	-	1.83
Fe	-	0.52
Na	-	12.60
Al	-	0.53
Si	-	28.00
Pb	3.47	-
Sn	1.28	

The XRD analysis was carried out using X-ray diffractometer modeled GBC Enhanced Mini Material Analyzer (EMMA). XRD pattern gives information relative to the nature and structure of the alloyed thin films of $SnPb_2O_4$ prepared at 60^0C of sodium hydroxide solutions show x-ray diffraction of the above listed alloyed thin films. The patterns show sharp and well defined peaks which indicates the crystalline nature of alloys of $SnPb_2O_4$. The crystallite sizes given in Table 3.3 are obtained using Debye-Scherers equation [12], given in equation (3.1)

$$D = \frac{k\lambda}{\beta Cos\theta} \qquad (3.1)$$

where k is the shape factor (k= 0.9), D is the grain size or average crystallite size, λ is the wavelength of CuKα radiation used (λ = 1.54Å, β is the experimentally observed diffraction peak width at half maximum intensity (full width at half maximum FWHM) and θ is the Bragg's diffraction angle.

3.2 Structural properties

Table 3.3 X-ray Diffraction Results of $SnPb_2O_4$, alloyed thin films

Sample A_{12}	2θ (degree)	d-spacing (Å)	FWHM (radian)	Grain size (Å)	Count	hkl
PbO: SnO_2	22.30	3.983	0.153	92.29	49	(111)

Figure 3.3, shows the XRD pattern of $SnPb_2O_4$ alloyed thin films of sample A_{12} with one diffraction peak of 49 at 2θ = 22.30^0. The pattern shows a well defined peak, which indicates the crystalline nature of the alloyed $SnPb_2O_4$ at 60^0C of NaOH solution. The average crystallite size for this alloy, was determined using equation 3.1, and is equal to 92.29nm with corresponding Miller indices (111). The XRD results, also show that a new compound alloyed thin film known as tin (iv) dilead oxide with orthorhombic crystal system was formed. It has a chemical formula; $SnPb_2O_4$. The lattice parameters of $SnPb_2O_4$ alloyed thin films of sample A_{12} are a = 8.709Å, b = 8.721Å and c = 6.292Å.
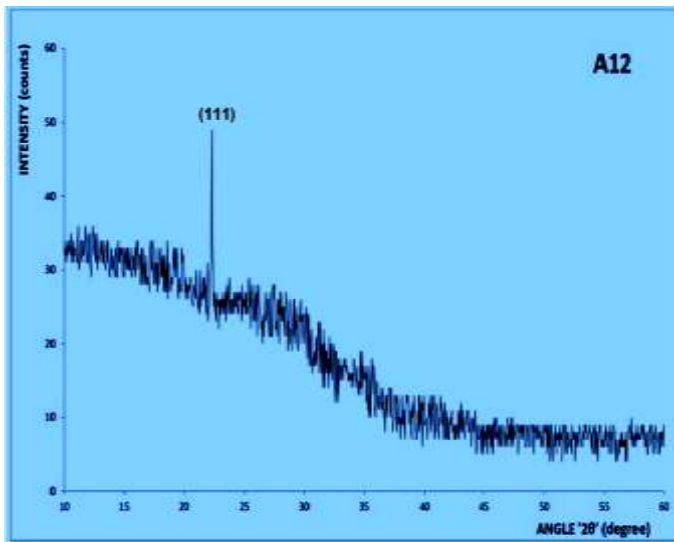
3.3 Microstructure of the deposited alloyed thin films

Microstructure of the thin films of $SnPb_2O_4$, were determined using electron microscope Phenom Prox, Model number MVEO16477830 manufactured by Phenom World Eindhoven Netherland. The process of analysis is through back scattering electron imaging method.

In Figure 3.4 and samples and A_{12} of $SnPb_2O_4$ has coarse but well defined cloudy and granular surfaces with grain size. This shows that sample has high porosity and roughness which may be due to vaporization of water [13].
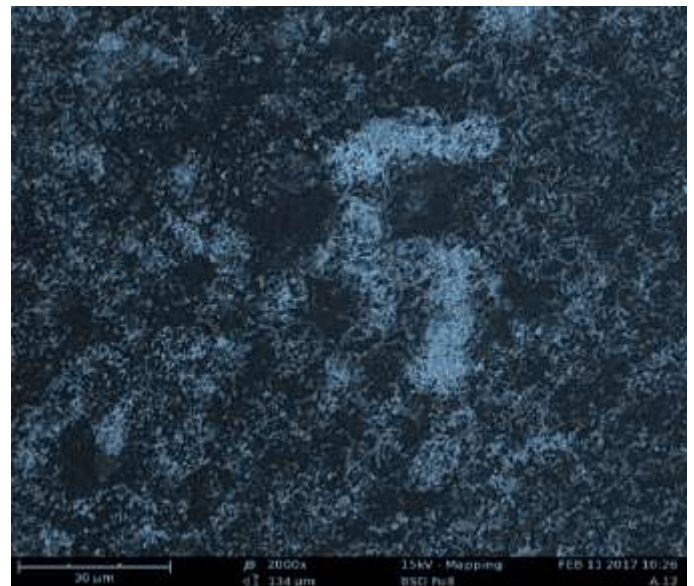

Figure 3.3 XRD Pattern of $SnPb_2O_4$ alloyed thin films of sample A_{12} at 60^0C of NaOH solution

Figure 3.4 Scanning electron microscopy of sample A_{12} of $SnPb_2O_4$ alloyed thin films

3.4 Optical properties

The optical properties of the deposited films were carried out using UV-1800 double beam spectrophotometer of wavelength range 190nm-1200nm. The transmittance spectra were measured directly from the spectrophotometer, other optical properties were determined using their appropriate equations. The transmittance spectrum shows that the films of samples A_{11} and A_{12} have good transparency in the UV (30%-65%) for sample A_{11} and good transmittance (27%-70%) for sample A_{12}. There are also high transmittances (65%-76%) for sample A_{11} and (70%-80%) for sample A_{12} in the visible region of electromagnetic spectrum. In the near-infrared region, samples A_{11} and A_{12} have very high transmittance (76%-80%) and (77%-75%) respectively; of the region of electromagnetic spectrum as shown in Figure 3.5. This makes these films good materials for UV filter [14]. This behavior of the two samples may be attributed to different annealing temperatures of 250^oC and 200^oC respectively for A_{11} and A_{12}.
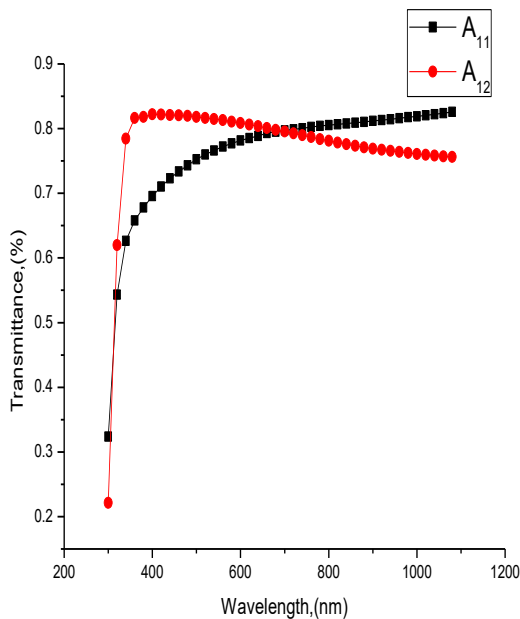

Figure 3.5 Graph of transmittance against wavelength for $SnPb_2O_4$ alloyed thin films of samples A_{11} and A_{12} at constant temperature of 60^0C of NaOH solution.

The graph of the reflectance in Figure 3.6, is obtained from the equation

$$R = 1 - (T + A) \qquad (3,2)$$

where R is the reflectance, A is the absorbance and T is the transmittance.

Samples A_{11} and A_{12} have low reflectance of 9% to 19% and 9% to 17% respectively as depicted in Fig.3.6, The reflectance decreased as the wavelength increases from the UV through the visible to the near infrared regions of electromagnetic spectrum. This makes $SnPb_2O_4$ useful in the area of multilayer

solar control coating. The coating allows the visible part of the spectrum in, but either reflects the infrared (IR) radiation back into the room (energy-saving) or does not allow the infrared radiation into the room (heat-protection) depending on which side of the window has the coating [14].This material can serve as front contact for solar cells and liquid crystal displays for optoelectronic applications. It could also be a good material for solar energy conversion for generation of electricity.
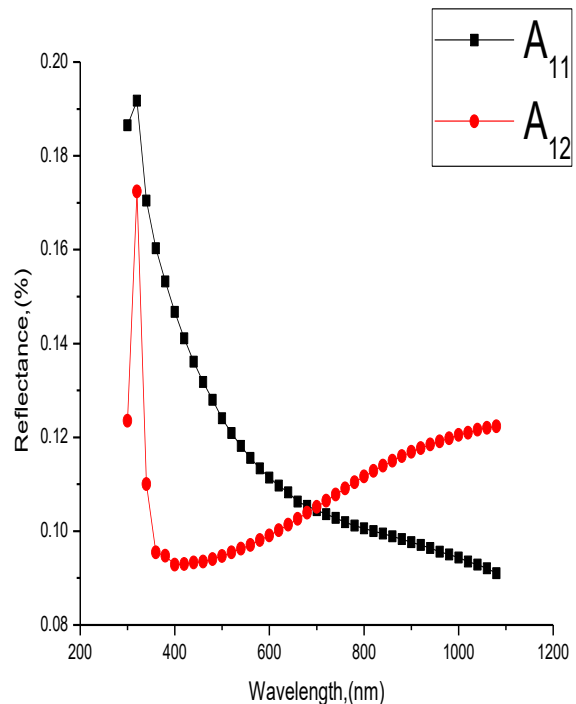

Figure 3.6 Graph of reflectance against wavelength for $SnPb_2O_4$ alloyed thin films of samples A_{11} and A_{12} at constant temperature of 60^0C of NaOH solution

The graph of the refractive index in Figure 3.7 is obtained from the equation,

$$n = \frac{1+\sqrt{R}}{1-\sqrt{R}} \qquad (3.3)$$

where n is the refractive index and R is the reflectance.

The refraction index of sample A_{11} rises from 2.5 at λ= 320nm to its maximum value of 2.6 at λ= 340nm and falls as wavelength increases until it reaches the minimum value of 1.8 at ʎ=1080nm. Sample A_{12} increased from 2.4 at λ= 320nm to its peak value of 2.6 at ʎ=340nm and decreases as wavelength increases up to λ=1080nm at n=1.8.The behaviour of these two samples of $SnPb_2O_4$ makes it possible for use in the area of multiple solar control coating applications where materials with high refractive index are required.
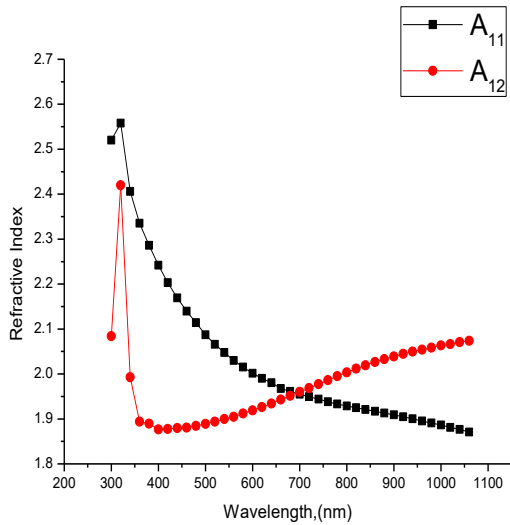
Figure 3.7 Graph of refractive index against wavelength for $SnPb_2O_4$ alloyed thin films of sample A_{11} and A_{12} at constant temperature of 60^0C of NaOH solution

In Figure 3.8, the optical energy band gap is obtained in k space from the relation

, $\qquad (\alpha h\upsilon)^2 = A (h\upsilon - E_g)$ $\qquad$ (3.4)

where A is a constant, hv is the photon energy E_g, is the energy band gap and α is the absorption coefficient.

The energy band gaps of samples A_{11} and A_{12} are evaluated by extrapolating the linear portion of the plot $(\propto h\upsilon)^2$ against hυ at αhυ = 0 where α is the absorption coefficient and hυ is the photon energy. A direct band gap value of 3.60 ± 0.05eV is obtained for sample A_{11}. Sample A_{12} has a direct band gap of 3.7 ± 0.05eV. The two samples have in average, energy band gap of 3.65 ± 0.05e V. The wide band gap obtained in this work makes the $SnPb_2O_4$ a good material for the production of laser diodes and light emitting diodes (LEDs) [15].
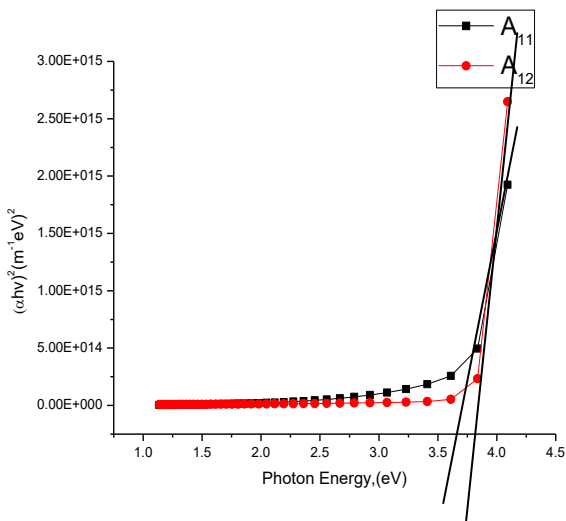

Figure 3.8 The Graph of $(\alpha h\upsilon)^2$ against photon energy hυ for $SnPb_2O_4$ alloyed thin films of samples A_{11} and A_{12} at constant temperature of 60^0C of NaOH solution.

Possible Applications

The deposited alloyed thin films with wide energy band gaps, high transparency in the UV, visible and near infrared regions can be found useful in the areas of Passive applications as dazzling coating, cold and heat windows, solar thermal-energy collector, selective absorbing layer.

Active applications:

solar cell applications, semiconductor materials, for optoelectronic applications, UV light emitting devices, sensors, and in optical communications.

V. CONCLUSION

$PbO:SnO_2$ alloyed thin films were deposited on glass substrates using two solution based methods: successive ionic layer adsorption and reaction and solution growth technique at constant temperature of 60ºC of NaOH solution while zinc complex ions were kept at room temperature of 20^oC. NH_3 solution was used as complexing agent.

The deposited samples were annealed between 100^oC-250^oC, using Master Chef Annealing Machine. The alloyed thin films exhibited high transmittance from the ultraviolet region, through the visible to near infrared regions of electromagnetic spectrum. Other optical properties of the samples were determined using appropriate equations. Direct average energy band gap of 3.65 ± 0.05e V. was obtained for $SnPb_2O_4$ alloyed thin films. The other properties investigated are absorbance, reflectance, optical conductivity, optical constants and absorption coefficient. From the XRD results, a new compound alloyed thin film known as tin (iv) dilead oxide with orthorhombic crystal system was formed.

These material alloy thin films prepared under this condition with wide energy band gap, high transparency in the visible region can be found useful in passive applications as dazzling coating, cold and heat windows, ceramics, solar thermal-energy collector, selective absorbing layer and active solar cell applications, semiconductor materials, for optoelectronic applications, UV light emitting devices, laser diodes, sensors, and optical communications etc. Also, these alloyed thin films prepared under this condition, have higher breakdown voltage, ability to sustain large electric field, low electronic noise, stable at higher temperature and high power operation. Due to their thermal stability, they can be found useful in the area of ceramics production, anti-corrosion material in iron and other metallic materials.

REFERENCES

[1]. S.L. Manish Comparative analysis of tractor's trolley axle by analytical method (by considering change in material and change in existing shape and size). *International journal of innovative and research development.* 4(1) 1-10 (2013).

[2]. M.T.S. Nair, A. Fernandez, M. Ocampo and P.K. Nair Prospects of Chemically Deposited Metal Chalcogenide Thin Films for Solar Control Applications, *Solar Energy Material and Solar Cell.* Vol. 4, pp. 829 – 835 (1988).

[3]. S. Han, H. Kwon, S. Kim, S. Ryu, W. Yun, D. Kim, J. Hwang, J. Kang, J. Baik, H. Shin Band-gap transition induced by interlayer van der waals interaction in MoS_2. *Journal of Physical Review.* 84 (4) 045 – 409(2011).

[4]. P. Johari and V. Shenoy Tuning the electronic properties of semiconducting transition metal dichalcogenides by applying mechanical strains. *Journal of ACS nanotechnology* 6 (6) 5449 – 5456 (2012).

[5]. X. Wu, P. Sheldon, Y. Mhathongdy, R. Rihelin, A. Mason, H.R. Moutino and T.J. Coult A.I.P. Conf. CPV Photovoltaic Review American Institute of Physics (1999).

[6]. S.J. Bu, Z.G. Jin, X.X. Liu, L.R. Yang, Z.J. Cheng Synthesis of TiO_2 Porous Thin Films by Polyethelene Glycol Templating and Chemistry of the Process. *J.Eur.Ceram. Soc.* 25(5), 673-679 (2005).

[7]. W.D. Callister, Materials Science and Engineering: An Introduction 7th edition, John Wiley and Sons, Inc. New York (2007).

[8]. J.D. Verhoeven, Steel Metallurgy for the Non-metallurgist. ASM International. p. 56 (2007).

[9]. F.C. Eze Electroless Deposition of CoO Thin Films. *J. Phys. D. Appl. Phys.* Vol. 31, pp.1-8 (1998).

[10]. J.I. Onwuemeka and N.C. Nwulu The study of the deposition, compositions and optical properties of CdO thin films at 60°C-100°C of NaOH solution and annealed at 200°C for 1hour and 3hours, prepared by Solution Growth Technique. *International Journal Of Innovative Research And Knowledge.* **2**(5) 29-35 (2017).

[11]. M. Reka, B. Devi. N. Lawrence, N.J. Prithirivikumaran Synthesis and characterization of conducting polymer polyaniline doped with salicylic acid. *International journal of Chem. Tech. Research,* 6(13), 5400-5403 (2014).

[12]. U. Cernigoj, U.L. Stangar, P. Trebse, U.O. Krasove, S. Gross, (2006), Photocatalytically Active Ti02 Thin Films Produced by Surfactant- Assisted Sol- Gel Processing. *Thin Solid Films*, 495 (1-2), 327-332 (2006).

[13]. J.I. Onwuemeka, O.K. Nwofor, N.C. Nwulu, I.E. Nwosu, F.M. Ezike and C.G. Obizo The optical study of ZnO thin films at different times of annealing and varying temperatures. *Journal of Applied Physics (IOSR-JAP).* PP. 47-51 (2014).

[14]. D C Look Recent Advances in ZnO Materials and Devices. *Mat. Sci Eng.* Vol.80, p 383 (2001).